

pVPD Technical Description

STAR TOFp Group

May 14, 2000

Abstract

This document describes the technical details of the pVPD Detector. The components of the pVPD that are the same as components used in the TOFp tray are described. The three design differences between the pVPD and TOFp are also discussed. These concern the mounting approach, the HV system, and magnetic field effects.

Contents

1	Introduction	2
2	Components common to TOFp and pVPD.	7
3	Mounting	7
4	PMT High Voltage	9
5	Shielding	9

List of Tables

1	pVPD Executive summary.	4
2	pVPD cable list.	6
3	The STAR fringe fields near the beam pipe and the pVPD.	9

List of Figures

1	Isometric view of a pVPD Detector Assembly. There are two of these - one on the East and one on the West.	2
2	A schematic overview of the pVPD connections. Only one of the two Detector Assemblies is shown.	5
3	Front view of a pVPD Detector Assembly.	8
4	Cutaway side view of the pVPD PMT Shielding.	10

1 Introduction

The present document describes the technical aspects of the “Pseudo Vertex Position Detector” (pVPD). This is a detector sub-system of the STAR Time-Of-Flight Patch (TOFp) System [1]. The single functional requirement of the pVPD is to provide timing start signals to the TOFp Racks with resolutions in the range 40-55ps. The technologies chosen for the pVPD were defined based on the following criteria. The system overall must be safe. The system overall must meet the physics requirements. The detector must impose the minimum possible thickness in terms of interaction and radiation lengths, as there may in the future be detectors “behind” the pVPD. The pVPD cannot mount off of, or even touch, the beam-pipe and it must allow for a certain amount of variability in the pipe’s absolute position with respect to a specific Aluminum I-beam. In the following, we provide the technical details on the pVPD detector that meets these criteria.

The pVPD System as a whole consists of two pVPD “Detector Assemblies,” and the cabling to connect each detector assembly to the platform. Each of the pVPD Detector Assemblies mounts near the beam-pipe and outside of the STAR pole tips, one on each side of STAR, at a $|Z|$ position near 4.5 m. An illustration of one of the pVPD Detector Assemblies is shown in Figure 1.

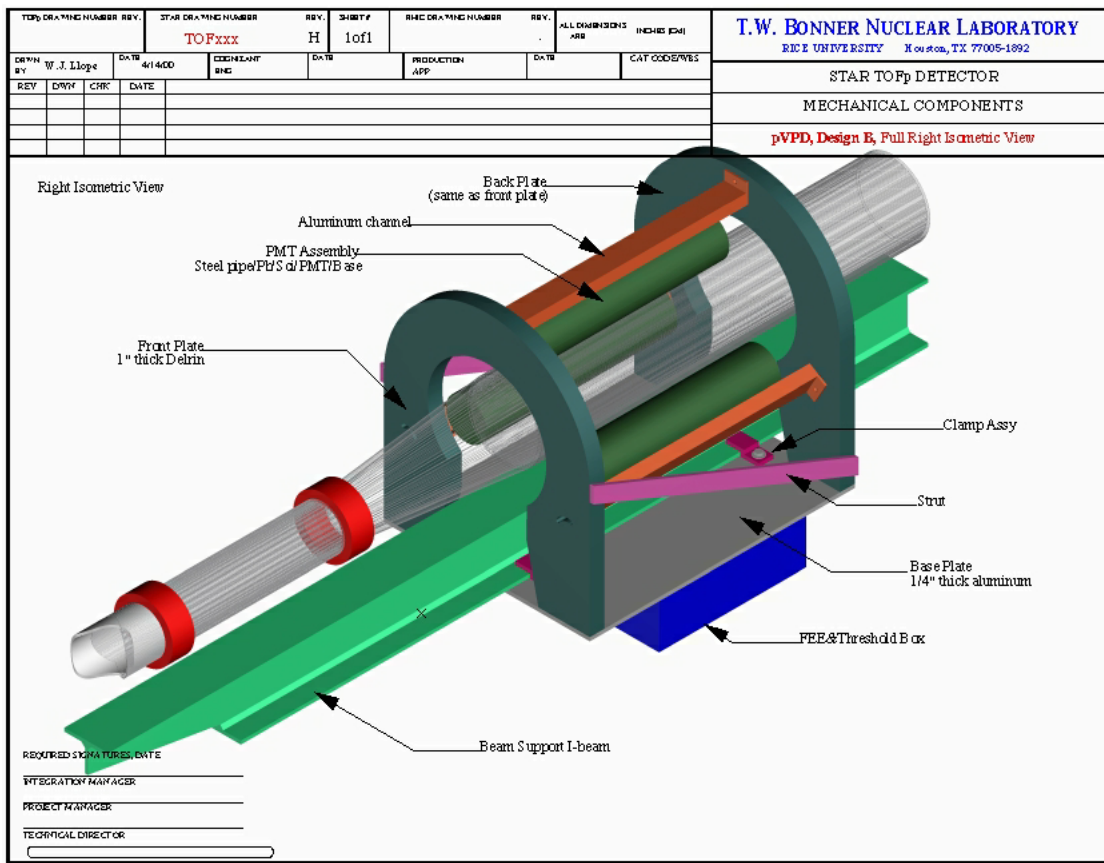


Figure 1: Isometric view of a pVPD Detector Assembly. There are two of these - one on the East and one on the West.

Each detector assembly consists of a mounting structure, three “PMT Assemblies,” and a small Front-End Electronics (FEE) box. The PMT Assemblies consist of a 1/4” thick layer of Lead and a 1 cm thick layer of fast plastic scintillator glued to a Hamamatsu R2083 2” PMT in a “flashlight” design. The PMTs are magnetically shielded, as the residual STAR magnetic fields are ~500 Gauss at $|Z| \sim 4.5\text{m}$. The pVPD FEE and Remote Threshold Systems are the same low-size and high-performance boards as used in the TOFp tray. The pVPD digitization is done in the TOFp rack. Coaxial cable of the RG-58 family carries the signals to the platform, where commercial CAMAC electronics (PS 706 discriminators, LeCroy 2228A TDC, and Lecroy 2249A ADC) do the final processing and digitization. The remainder of the pVPD cabling consists of the “LV Bus”, the “Threshold Control” cables and SHV cables for the PMT base high voltage.

The performance of such a pVPD was studied in detail in full STAR simulations [2]. It was observed that a simple 6 channel system performs very well in RHIC heavy-ion collisions given the very high multiplicities of very forward and very fast particles. The start-timing resolution of individual pVPD channels is expected to be ~ 50 ps or better in Au+Au collisions at any impact parameter, and in Si+Si collisions at impact parameters less than ~ 5 fm.

Table 1 provides a general summary of the pVPD System parameters and requirements. Shown in Figure 2 is a schematic overview of all of the connections to the detector. Table 2 provides a listing of the TOFp cabling and ratings. Quite a few of the components of the pVPD are the same as those used in the TOFp tray. Thus, most of the pVPD electronics chain has already been reviewed and deemed compliant with BNL/RHIC safety regulations. These common areas will be discussed first below. The major differences between the TOFp and pVPD systems fall into three categories - the mounting approach, the PMT Voltage system, and the existence of magnetic shielding. These areas are discussed below in sections 3, 4, and 5, respectively.

Table 1: pVPD Executive summary.

Requirement	Specification	Comments
Detector Assembly		
Converter	6	Lead, 1/4" thick
Scintillator	6	Bicron BC420, $2.5 \times 2.5 \times 1 \text{ cm}^3$
PMTs [†]	6	Hamamatsu R2083, 3 PMTs/subdetector
HV Bases	6	Linear resistive, HV from CTB's Lecroy 1440
Shields	6	five-layer, O.D. 2.75", length 13"
Structure	2	Delrin and Aluminum construction
FEE Boards [†]	2	Rice Ver. 7, 1 board/Detector Assy
Thresh. Interface [†]	2	Rice Ver. 2, 1 board/Detector Assy
Geometry		
Configuration	2×3	number of PMTs
Pipe Clearance [‡]	3/8"	see Figure 3
Envelope I.R.	5 3/8"	see Figure 3
Envelope O.R.	7"	see Figure 3
Z Front	4.4m	
Z Back	4.9m	detector is 18" long in Z
Connections		
Signal cables [†]	12	6(6) for ADC(TDC), coaxial, $\leq 100'$ long
Max Cable Attn	20 dB/100m @ 200 MHz	
Max Ampl X-talk	0.1%	
Max Time X-talk	10ps	
Low voltage bus [†]	4 conductor	100 ft long, for +5 and -5.2 V power to FEE
Thres. bus [†]	5 conductor	100 ft long, for control/readback of Thresh. Sys.
Heat removal	air in WAH	pVPD is outside STAR pole tips and in the open
Digitization		
FEE Time resn. [†]	<20ps	Pulser input (constant pulse height)
FEE Time resn. [†]	<60ps	1 mip-like laser input, far-end hits
ADC/TDC modules [†]	CAMAC	Lecroy 2228A and 2249A
ADC resolution [†]	>10 bits	
TDC resolution [†]	>10 bits	
TDC conversion [†]	$\leq 50 \text{ ps/bin}$	
TDC full scale [†]	100 ns	
Digitization time	$\leq 100 \mu\text{s}$	fast clears used
Power, Bases	6 W nom.	1 W/base for 6 bases (over 6 separate cables)
Power, FEE [†]	3.6W nom.	0.6 W/ch for 6 chs (over 2 separate LV Buses)
Power, Total	10 W	

[†] Same as in the TOF_p Detector.[‡] See section 3.

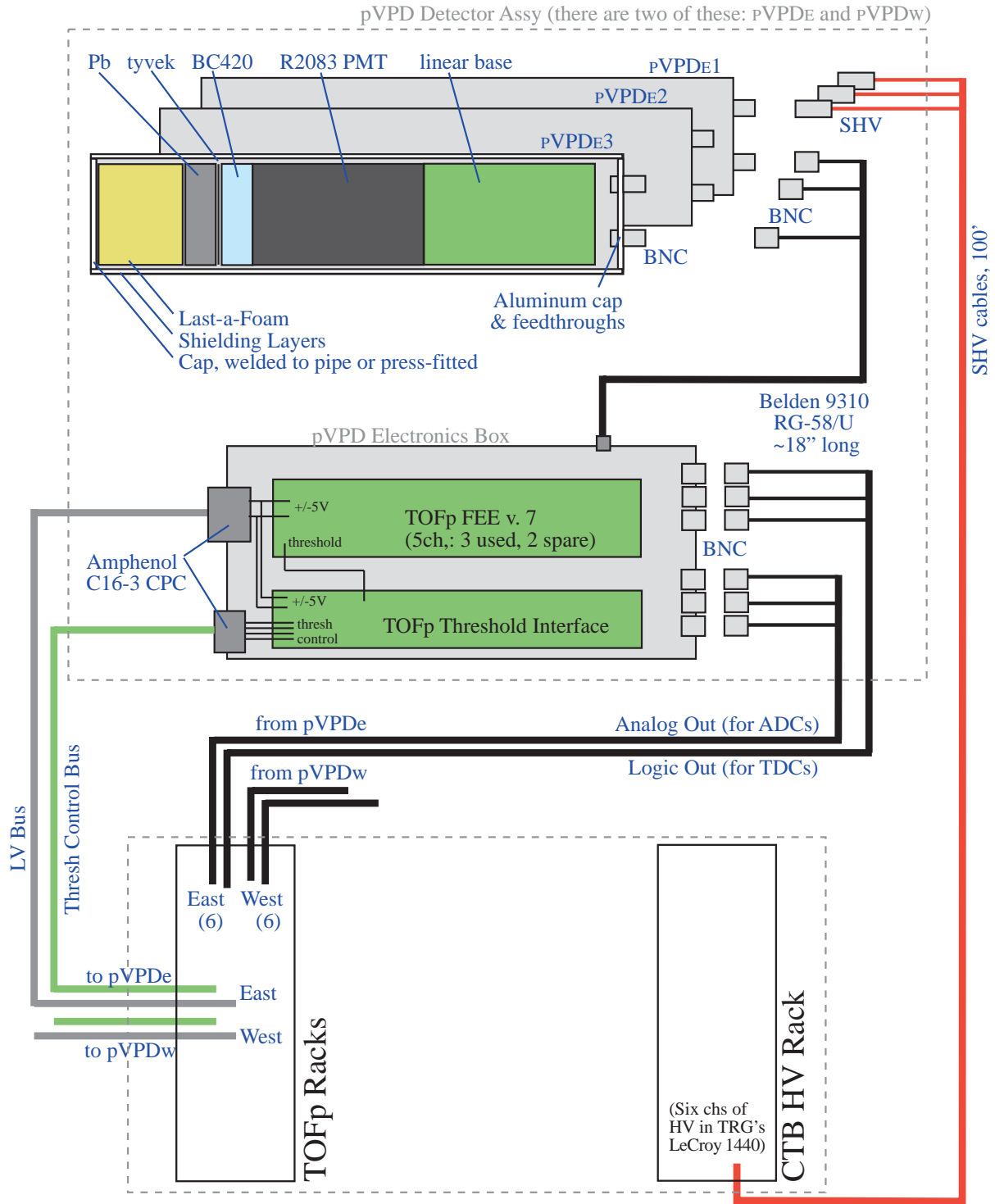


Figure 2: A schematic overview of the pVPD connections. Only one of the two Detector Assemblies is shown.

Table 2: pVPD cable list.

	No.	Type	Product	Voltage (V)		Current (A)		
				Oper.	Rated	Nominal	Fault	Rated
Cables								
Signal	12	RG-58/U Coaxial	Belden 9310	0.8	300			
High Voltage	6	RG-59/U	Belden	2000	5000			
Threshold bus	1	12 pair, 18 AWG	Belden 9747	0.5	300	0.01/pr		
Low voltage bus	1	5 cond., 16 AWG	Belden 9954	±5	600	8	10	
Lead wire	5	16 AWG, Teflon	Belden 83030	±5	1000	8	10	
Connectors								
FEE→RG-58/U	6	Lemo	Lemo USA	0.8	700			4
LV→pVPD	1	5+PE cond.	Amp C16-3	±5	400	8		21
LV→FEE	4	5 pin	Weidmuller LM3.50/135	±5	300	8		10
Threshold Bus	1	6 cond. CPC	Amp 737097	0.5		0.01		

2 Components common to TOFp and pVPD.

The components of the pVPD that are the same as TOFp components are discussed in this section. These components have already been successfully reviewed [3] for compliance with BNL/RHIC safety regulations.

The Front End Electronics for the pVPD are the custom Leading Edge Discriminator boards developed at Rice for TOFp without modification. These are five channel boards that include properly rated connectors as well as fusing on both low voltage inputs to each board. For the pVPD implementation, only three of the five channels are used, leaving two per board as spares.

The Low Voltage and Remote Threshold System is also the same as that developed for TOFp. The connectors and cabling used to connect the FEE and Threshold Systems to low voltage and to control the remote threshold are the same as those used in the TOFp detector.

The current draws on the (two) LV Bus cables for the pVPD are roughly $1/10^{th}$ of those on the TOFp LV bus. This is because each LV Bus in the pVPD System drives only a single Rice v.7 FEE board, whereas the TOFp LV Bus these drives ten of these boards.

The cables and their ratings are tabulated in Table 2.

3 Mounting

At roughly 4.2m, there is a “neck-down” from the 5” O.D. beam pipe to flanges and bellows linking to the 3” O.D. pipe that passes through STAR. All of this is supported by fittings that stand off a 4” Aluminum I-beam which is attached to the walls of the WAH. Positioning the pVPD in this region is attractive because the real estate is uniform over long distances and is relatively more accessible than STAR detectors inside the pole tips. No cooling water path near the pVPD is needed as the power dissipation is low and detector elements are in the open in an air-conditioned room. The existing I-beam provides the necessary mounting points, and no modification to existing pipe-related hardware is needed. The residual STAR magnetic fields are low enough that non-mesh PMTs can be used, given appropriate shielding (see section 5).

The simulations [2] implied excellent pVPD performance over a range of pVPD PMT Assembly positions in both $|Z|$ and $|R|$, but the best performance overall is obtained in general with the PMT Assemblies as close as possible to the beam pipe radially. However, it is important to note that the pipe support fittings intentionally allow for adjustments (in two dimensions) of the position of the pipe with respect to the I-beam. The weight of the present pipe causes the free end of the I-beam to sag by 0.2” at its end. The pipe as mounted off of the I-beam is then surveyed and the fittings are adjusted by RHIC to move the pipe back on line (up 0.2” with respect to the I-beam). The addition of a pVPD Detector Assy on the same I-beam would cause an additional sag.

We estimate that each pVPD Detector Assy will weigh $3 \times 10 + 10$ lbs, or 40 lbs/Det Assy. The sag to the I-beam caused by putting another weight on the I-beam at $|Z| \sim 4.2\text{m}$ was calculated by Ralph Brown [4]. He used 80 lbs (*i.e.* a safety factor of two for the weight) at $|Z| \sim 4.2\text{m}$ and estimated the I-beam sag would be 0.1”. This is, quote [4], well within the range that can still be compensated for easily using the pipe support fittings. The pVPD Installation Plan thus involves scheduling with RHIC so that their (~ 0.05 ”) pipe adjustment to compensate for the actual pVPD weight occurs at the appropriate stage of the pVPD installation.

While the pipe is by design adjusted so that it is correctly absolutely positioned, the weight of the pipe on the I-beam causes the I-beam to point below parallel when looking towards $|Z|=0$. This amounts to an angle of 0.3 degrees at the end of the I-beam.[4] No justification for compensating for this tiny angle in the pVPD mounting structure was seen.

The front view of the detector assy depicting the relevant hardware during installation is shown in Figure 3. The pVPD Base Plate and Clamp Assys are first removed from the two Detector Assys. Also, the two lower PMTs are rotated “up” from the axis of the detector and locked down in that position. Once approved for installation and given the existence of platforms near the pipe at $|Z| \sim 4.5\text{m}$, the pVPD Installation proceeds via the following steps. As there are two pVPD Detector Assys, these steps are followed twice, once on each side of STAR.

- Turn STAR magnetic field on.
- Measure field with simple probe at 1-2 locations on back of FTPC.

- Turn STAR magnetic field off.
- Install Base Plate to underside of I-beam using Clamp Assy hardware.
- Tighten down lock screws to secure $|Z|$ position of Base Plate.
- Install two 20 lb weights on Base Plate, one on each side of I-beam.
- RHIC surveys pipe location and repositions to compensate for ($\sim 0.05''$) sag.
- Remove weights.
- Lower detector superstructure from above onto Base Plate, and bolt down.
- RHIC resurveys to check pipe position still correct.
- Rotate two lower PMT Assys down and into position, and lock down.
- Install FEE Box and cabling between FEE box and PMT Assys.
- Install cabling from pVPD Det Assy to Platform (TOFp Racks and CTB HV Rack).
- Install proper Lock-Out/Tag-Out documentation and obtain clearance to power up pVPD.
- Turn STAR magnetic field on.
- Measure field with simple probe at 1-2 locations on back of FTTPC, and compare to values from step 2.
- Begin pVPD commissioning using cosmics.

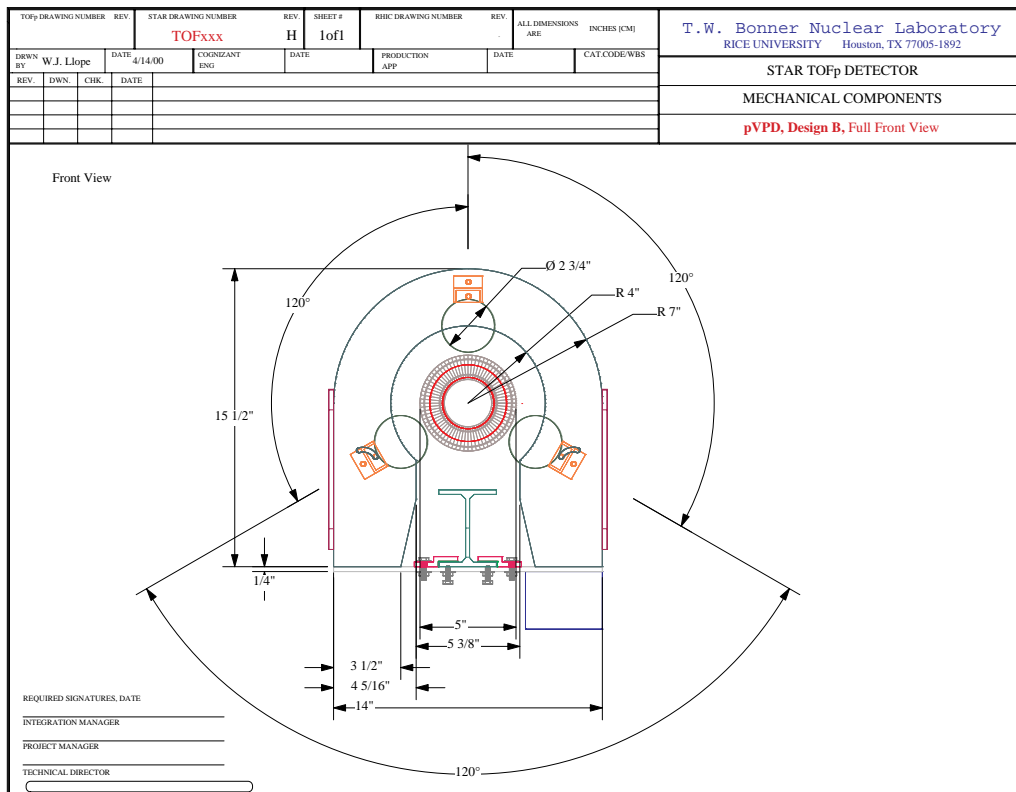


Figure 3: Front view of a pVPD Detector Assembly.

4 PMT High Voltage

In the CTB, the PMT voltage system consists of a Lecroy 1440 mainframe delivering high voltage over long cables to simple resistive bases inside the CTB trays. For the pVPD, spare channels of the same 1440 and SHV cabling is used to provide high voltage to the PMTs. This highly conventional approach was adopted because of the availability of existing PMTs and Bases (read “free”) and the availability of the spare channels of the existing CTB HV System.

The HV cabling is standard RG-59/U with a red jacket and SHV connectors, such as available from BNL stores and is recommended in Ref. [5]. The typical anode voltages for pVPD PMTs is 2 kV. Further information can be found in Table 2 and Ref. [5].

5 Shielding

To take advantage of the cost and development savings of using a conventional HV-based PMT bases, the residual magnetic fields near the pVPD PMTs must be suppressed. This is as usual done with layered magnetic shielding, which is described in this section.

The STAR field has been mapped including fringe regions so the field strengths along two axes (R and Z) in the area being considered for the pVPD are known. These values are shown in Table 3.

Table 3: The STAR fringe fields near the beam pipe and the pVPD.

Z (cm)	R (cm)	B_z (Gauss)	B_r (Gauss)
400	0	972	0
450	0	482	0
500	0	291	0
550	0	190	0
400	25	915	195
450	50	423	119
500	50	273	61
550	50	182	38

It is possible effectively shield PMTs up to approximately one kGauss. That implies that a fully functional pVPD could be constructed based on our knowledge of effective shielding techniques for any of the values of Z and R in the ranges shown in Table 3. However, a considerable thickness of steel and mu-metal layers are needed if one wants to position the pVPD near $|Z| \sim 4\text{m}$ where the fields indeed approach 1 kG.

However, the full simulations [2] imply that the pVPD performance in A+A collisions is adequate over a wide range of Z positions from ~ 4 to ~ 5.5 m. By moving the pVPD back from $\sim 4\text{m}$ to $\sim 5\text{m}$, the thicknesses and lengths of the shield components can be reduced. This decreases the total amount of material in the detector which lessens its shadow on detectors which may sit eventually “behind” the pVPD. It also reduces the total weight of the Detector Assy which loosens the requirements on the mounting structure and lessens the sag in the I-beam caused by mounting the pVPD off of it.

We have therefore adopted a lighter and less dense shielding approach that will be adequate for pVPD $|Z|$ positions greater than $\sim 4.5\text{m}$. This approach is shown in Figure 4.

The Shielding extends beyond the front face of the PMTs by about 2”. The innermost layer is a 16 mil thick layer of μ -Metal, as made from four 4 mil thick layers. This layer is at photocathode potential and is both the first layer of magnetic shielding and also the electrostatic shield. The second layer is an Insulating Sleeve (“Co-netic” by Perfection Mica Inc.). The third layer is a 40 mil thick cylinder of Iron/Nickel Alloy. The fourth layer is another insulating sleeve. The fifth and outermost layer is a 3/16” thick cylinder of Steel. This layer is at ground potential.

The cap is thick (1/4”) which reduces the length of the shields in front of the PMT photocathode, and serves as additional converter for the (predominantly) photon flux along the beam pipe that causes pVPD hits. It is attached to the outer steel layer in a mechanical joint (press-fitting) or, if can be achieved, very-low carbon welding.

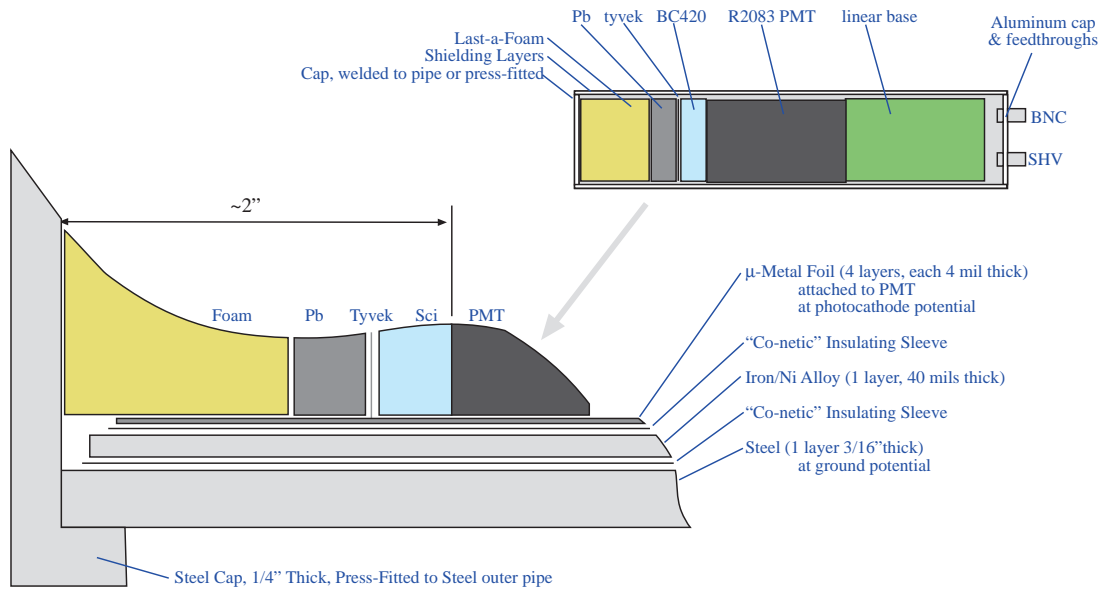


Figure 4: Cutaway side view of the pVPD PMT Shielding.

The outer Steel layer is attached to support pieces called “boats” which run the length of the pVPD between the front and back plates. The boats are 1 1/2” architectural channel, and simple hose clamps are used to hold the PMT Assy to the boats.

There is a distance of 1.5 meters between the back face of the FTFC and the front face of the pVPD, which is roughly an order of magnitude larger than needed to insure the pVPD shielding does not modify the local fields inside the FTFC. Nonetheless, the Installation procedure described in Section 3 includes comparisons of the local magnetic field at the back face of the FTFC with the field on and the pVPD either in or out.

References

- [1] <http://bonner-mac8.rice.edu/~TOF/default.html>.
- [2] W.J. Llope, John Mitchell, and F. Geurts, STAR Note 416, 3/16/2000.
- [3] The TOFP Systems were reviewed by the BNL Safety Committee, Y. Makdisi *et al.*, on 12/16/1999.
- [4] R. Brown, private communication, 4/13/2000.
- [5] H. Matis and B. Minor, STAR Note 378 (1998).